Stem Cell Research (2013) 11, 782–792

Available online at www.sciencedirect.com

SciVerse ScienceDirect

www.elsevier.com/locate/scr

Megakaryocytes co-localise with hemopoietic stem cells and release cytokines that up-regulate stem cell proliferation

Shen Y. Heazlewood[a,1], Rebecca J. Neaves[b,1], Brenda Williams[a], David N. Haylock[a,b], Timothy E. Adams[a], Susan K. Nilsson[a,b,*]

[a] Materials Science and Engineering, Commonwealth Scientific and Industrial Research Organization, Melbourne, Australia
[b] Department of Anatomy and Developmental Biology, Monash University, Melbourne, Australia

Received 22 February 2013; received in revised form 23 April 2013; accepted 14 May 2013
Available online 28 May 2013

Abstract We report transplanted hemopoietic stem cells (HSC) preferentially lodge within two cells of mature megakaryocytes (MM). With both populations comprising ~0.2% of bone marrow cells, this strongly suggests a key functional interaction. HSC isolated from the endosteum (eLSKSLAM) showed significantly increased hemopoietic cell proliferation while in co-culture with MM. Furthermore, eLSKSLAM progeny retained HSC potential, maintaining long-term multi-lineage reconstitution capacity in lethally ablated recipients. Increased hemopoietic cell proliferation was not MM contact dependent and could be recapitulated with media supplemented with two factors identified in MM-conditioned media: insulin-like growth factor binding protein-3 (IGFBP-3) and insulin-like growth factor-1 (IGF-1). We demonstrate that HSC express the receptor for IGF-1 and that IGF-1/IGFBP-3 induced increased hemopoietic cell proliferation can be blocked by an anti-IGF-1 neutralising antibody. However, co-cultures of 8N, 16N or 32N MM with eLSKSLAM showed that MM of individual ploidy did not significantly increase hemopoietic cell proliferation. Our data suggests that MM are an important component of the HSC niche and regulate hemopoietic cell proliferation through cytokine release.

Introduction

In adults, hemopoietic stem cells (HSC) reside in bone marrow (BM), where they maintain hemopoiesis. Schofield et al. initially hypothesised that HSC reside in specific three-dimensional structures from which they coined the term "niche" (Schofield, 1978). It is these niches that provide the extrinsic cues controlling HSC fate. The molecular and cellular compositions of the HSC niche are under intense investigation and several cell types have been shown to be important HSC regulators; osteoblasts (OB), endothelial cells, CXCL-12 abundant reticular cells, neuronal cells as well as Nestin$^+$ mesenchymal stromal cells (reviewed in Shen & Nilsson, 2012). These cells secrete factors such as osteopontin, tenascin-C and hyaluronan which influence HSC fate (Nilsson et al., 2003, 2005; Stier et al., 2005; Grassinger et al., 2009; Ellis et al., 2011; Nakamura-Ishizu et al., 2012).

Although mature megakaryocytes (MM) residing within BM are primarily responsible for platelet production, they have recently been shown to directly and indirectly influence the BM microenvironment. Interleukin (IL)-6 released by MM

* Corresponding author at: CSIRO, CMSE, Bag 10 Clayton South MDC, Melbourne, Victoria 3169, Australia.
E-mail address: susie.nilsson@csiro.au (S.K. Nilsson).
[1] Equal contribution.

1873-5061/$ - see front matter.
http://dx.doi.org/10.1016/j.scr.2013.05.007

stimulates long-lived plasma cells (Winter et al., 2010) and is also known as a HSC regulatory cytokine (Suzuki et al., 1989; Jiang et al., 1994). Indirectly, MM influence HSC by regulating OB, stimulating their proliferation and differentiation while inhibiting osteoclast formation (Lemieux et al., 2010; Ciovacco et al., 2010; Kacena et al., 2004, 2006; Bord et al., 2005; Beeton et al., 2006). MM are also a major source of factors such as thrombospondin, platelet-derived growth factor and basic fibroblast growth factor-2, which are important in the regulation and recovery of vasculature and OB following BM damage (Kopp et al., 2006; Dominici et al., 2009). In addition, MM endocytose cytokines such as insulin-like growth factor (IGF)-1 and insulin-like growth factor binding protein (IGFBP)-3 for later release (Chan & Spencer, 1998). There are two members within the family of IGFs (IGF-1 and IGF-2) and six members within the IGFBP family (IGFBP-1 to -6) (Martin & Baxter, 2011). Recently, IGF-2 and IGFBP-2 secreted by foetal liver $CD3^{+}Ter119^{-}$ cells and tumorigenic cell lines were shown to increase HSC proliferation (Zhang & Lodish, 2004; Huynh et al., 2008, 2011). Due to the many different ways in which MM can influence the BM microenvironment, we investigated the role of MM in HSC biology.

Materials and methods

Mice

C57Bl/6 and PTPRCA congenic mice were purchased from Monash University Animal Services (MAS, Monash University, Australia). Red fluorescence protein (RFP) mice were bred at MAS. All animals were used at age 6–8 wks and all experiments were approved by Monash Animal Research Platform Ethics Committee.

Stem cell isolation

Murine hemopoietic stem cells were isolated as previously described (Nilsson et al., 2005; Grassinger et al., 2010). Briefly, iliac crests, femurs and tibias were excised, epi- and metaphyseal regions removed and bone shafts flushed to collect central (c) BM. Empty bones were pooled with epi- and metaphyseal regions and crushed prior to collagenase I and dispase II digestion for the isolation of endosteal (e) BM. BM mononuclear cells, isolated by density centrifugation (Nycoprep, Axis-Shield, Norway), were lineage-depleted based on lineage-restricted marker expression (B220, Mac-1, Gr-1 and Ter119) using Dynal beads (Life Technologies, USA). Lineage negative (Lin^{-}) cells were stained with anti-Sca-1-Pacific Blue and anti-c-Kit-AF647 for hemopoietic progenitor cell isolation (LSK: $Lin^{-}Sca\text{-}1^{+}c\text{-}Kit^{+}$), and anti-CD150-PE and anti-CD48-FITC for HSC isolation (LSKSLAM: $Lin^{-}Sca\text{-}1^{+}c\text{-}Kit^{+}CD150^{+}CD48^{-}$). Unless otherwise specified, all antibodies used in this project were from BD Biosciences or Biolegend (USA). Flow cytometry work was performed at FlowCore (Monash University) using influx cell sorters or LSRII analysers (BD Biosciences). FACS analysis was performed using Flow Jo software (Tree Star Inc., USA). Cell counts were performed on Sysmex KX-21N automated cell counter (Sysmex, Japan).

Megakaryocyte isolation

Megakaryocytes were isolated as recently described (Heazlewood et al., 2013). Briefly, central marrow was collected and depleted for lineage expressing cells (B220, Mac-1 and Gr-1) prior to staining with anti-CD41-FITC. Hoechst33342 (Life Technologies, USA) was used at 10 μM to identify MM of different ploidy. MM were isolated as side scatter $(SSC)^{high}$, $CD41^{bright}$ cells through a 100 μm nozzle at ~5000 cells/s and 20 psi. Due to both cell size and high CD41 expression, logarithmic scales were used with a decreased FITC voltage setting.

Cell culture

One hundred LSKSLAM cells and 100 MM were cultured in 100 μl of Iscove's Modified Dulbecco's media (IMDM, Life Technologies) supplemented with 1% bovine serum albumin (BSA) (Sigma-Aldrich, USA) and recombinant human insulin (10 μg/ml, Novartis, Switzerland), human transferrin (100 μg/ml, Roche, USA), human low density lipoprotein (3 μg/ml, MP Biomedicals, Australia), L-glutamine (2 mM/ml, Life Technologies), human IL-11 (100 ng/ml, Chemicon, Australia), mouse stem cell factor (10 ng/ml, Chemicon), human IL-6 (10 ng/ml, Peprotech, USA), human FLT-3 ligand (10 ng/ml, Apollo Cytokine Research, Australia), mouse IL-3 (133 U/ml, Immunex Corporation, USA), human thrombopoietin (TPO) (5 ng/ml, Apollo Cytokine Research), with or without mouse IGFBP-3 (775-B3), mouse IGF-1 (791-MG) or anti-mouse IGF-1 neutralising antibody (AF791) (R&D Systems, USA). After 6–7 days of incubation at 37 °C in an 85% nitrogen, 10% carbon dioxide and 5% oxygen humidified incubator, cells were counted and stained with anti-CD3-Pacific Blue, anti-B220-Pacific Blue, anti-B220-FITC, anti-Gr-1-FITC and anti-Mac-1-FITC. MM-conditioned media (CM) was collected from wells containing prospectively isolated MM cultured alone in the above media. "Aged media" was media collected after 6–7 days in culture without MM.

Cytokine array

Analysis using a custom mouse cytokine array (RayBiotech, USA) was performed following the manufacturer's specifications except for being adapted for analysis using the Li-Cor Odyssey Infra-Red Imaging System (Li-Cor Biosciences, USA). Briefly, membranes were blocked in Odyssey blocking buffer supplemented with 0.05% Tween-20 before incubation in control media or MM-CM, followed by biotin-conjugated antibody before incubation with IRDyeTM 800CW-streptavidin and visualization.

BM fluid collection

BM fluid from central BM was collected by flushing femurs using 200 μl of 50 mM Tris–HCl (pH 7.4), 150 mM NaCl, 1 mM EDTA with 1× complete protease inhibitor cocktail (Roche, Germany), 0.001 M PMSF and 0.001 M Na_3VO_4 (BM flush). Empty femurs were crushed in 400 μl of the same buffer and BM fluid collected (BM crush). BM fluids were centrifuged at 400 *g* for 5 min and used fresh for ELISA analysis.

Analysis of IGFBP-3 secretion

IGFBP-3 secretion was assessed by ELISA using a custom mouse IGFBP-3 ELISA kit (RayBiotech). Diluted kit standard, control media or MM-CM was incubated in 96-well plate strips and labelled for detection at 450 nm using an EnSpire 2300 Multilabel Reader (Perkin Elmer, USA). The CM from 2000 prospectively isolated MM was assayed. It should be noted that culture medium, and hence CM, was generated using Sigma BSA, which, unlike a number of other BSA sources, does not contain IGFBP-3 fragments (Twigg et al., 2000).

Homing and spatial distribution assay

The homing and spatial distribution of central/endosteal LSKSLAM cells was assessed as previously described (Grassinger et al., 2010). Briefly, cells were stained with 0.5 μM carboxyfluorescein diacetate succinimidyl ester (CFD-A/CFSE, Life Technologies) or 1 μM seminaphthorhodafluors-1 carboxylic acid acetate succinimidyl ester (SNARF-1, Life Technologies), pooled together with 2×10^5 whole BM filler cells from C57Bl/6 mice and transplanted intra-venously into non-ablated recipients. SNARF and CFSE were used interchangeably on the different populations in different experiments to negate any possible effect seen due to the dyes themselves. Fifteen hours post-transplant, BM from one iliac crest, femur and tibia was analysed on a LSRII to determine the homing potential of transplanted ($CFSE^+$ versus $SNARF\text{-}1^+$) cells. Total BM homing was calculated based on the assumption that one iliac crest, femur and tibia accounts for 15% of total BM (Smith & Clayton, 1970). The other set of leg bones were perfusion-fixed with 4% paraformaldehyde/0.1% gluteraldehyde at physiological pressure, excised, decalcified with 10% EDTA and embedded in paraffin. Three micron serial sections were cut, de-waxed and mounted in Vectashield fluorescence mount media (Vector Laboratories, USA) before alternate sections were scored using a fluorescence microscope with a UV/FITC/Texas Red triple dichroic filter to allow for the simultaneous visualization of $CFSE^+$ (green) and $SNARF\text{-}1^+$ (red) cells.

Long-term reconstitution assay

Limiting dilution analysis of donor cells was used to measure the frequency of cells that possess long-term multi-lineage reconstitution potential (Grassinger et al., 2010). Lethally irradiated recipients (split dose of 5 Gy each, 4 h apart) were intra-venously transplanted with the progeny of 3, 10, 30 or 100 eLSKSLAM either cultured alone, or co-cultured with MM. Cultured cells were pooled with 2×10^5 irradiated (15 Gy) whole BM filler cells from C57Bl/6 mice for injection. Hemopoietic reconstitution was assessed by lineage analysis of the peripheral blood (PB) at 6, 12 and 20 wks post-transplant with the addition of BM at 20 wks post-transplant. Following red blood cell lysis, PB was stained with anti-CD3-Pacific Blue, anti-B220-Pacific Blue, anti-B220-APC, anti-GR-1-APC and anti-MAC-1-APC for flow cytometry analysis. Mice with a greater than 1% donor reconstitution and B-cell, T-cell and myeloid cell lineages were identified as having been transplanted with HSC with long-term multi-lineage reconstitution potential. The frequency of long-term repopulating cells in each donor cell population was calculated using L-Calc Software (Stem Cell Technologies, Canada).

Real-time PCR

RNA was extracted from cells using Trizol (Life Technologies) and DNase-treated with TURBO DNA-free Kit (Ambion, USA) before reverse transcription with SuperScript III (Life Technologies) as per the manufacturer's instructions, using 100 ng of RNA. All pre-formulated TaqMan gene expression assays (containing unlabeled PCR primers and FAM dye-labelled TaqMan MGB probe) were purchased from Applied Biosystems (USA). Real-time PCR was performed using a 7500 Real Time PCR System (Applied Biosystems) using TaqMan Universal PCR mix (Applied Biosystems) with mouse β-actin as the endogenous control.

Identification of growth factor receptors on stem cells

Anti-IGF-1R antibody was purchased from Abcam (ab32823, UK) and anti-EGFR antibody was purchased from R&D (HXO01, USA). Stem cells were sorted as above, stained with 10 μg/ml of primary antibody or appropriate IgG control (BD Biosciences or R&D) before visualization with 2 μg/ml of anti-AF488 secondary antibody (Life Technologies) via flow cytometry.

Immunohistochemistry

Perfusion fixed murine femoral sections were stained with anti-mouse antibodies for anti-c-Mpl (the receptor for TPO) (1 mg/ml, clone N-20, R&D, USA), anti-IGFBP-3 (5 μg/ml, Clone 138202, R&D) or appropriate IgG isotype control (BD Biosciences or R&D). To enhance the signal, staining was amplified using a tyramide signal amplification fluorescence system kit as per the manufacturer's instructions (Perkin Elmer). Briefly, primary antibodies were detected with 1 μg/ml of biotinylated secondary antibody, then subsequently stained with SAV-HRP followed by FITC-conjugated tyramide for 6 min at RT. Sections were counter-stained with 4,6-diamidino-2-phenylindole (DAPI, Life Technologies) before been mounted in Vectashield fluorescence mounting media. MM were scored as endosteal if within the epi- or metaphyseal regions of the bone or less than 12 BM cell diameters from the bone:BM interface. This distance was arbitrarily defined based on the furthest distance of cells of donor origin 6 months post-transplant in non-ablated recipients (Ellis et al., 2011; Grassinger et al., 2010; Nilsson et al., 1997; Haylock et al., 2007).

Microscopy

Fluorescent cell cultures were visualized with an Olympus IX71 microscope and images were acquired with an Olympus U-CMAD3 camera. Fluorescently stained BM sections were visualized using an Olympus BX51 microscope and images were captured using an Olympus DP70 camera. A subset of images was acquired using a DotSlide microscope (Olympus, Germany). Light microscopy was performed on either a BX41 or CKX41 microscope (Olympus, Japan).

Statistical analysis

Differences between sample groups were evaluated by Mann–Whitney or one-way analysis of variance tests where appropriate using GraphPad Prism (GraphPad Software, USA) or SigmaPlot (Systat Software, USA). Data is presented as the mean ± SEM.

Results

MM are randomly distributed and transplanted HSC preferentially lodge within two cells of MM

Analysis of the distribution of large, polyploid MM identified using an anti-c-Mpl antibody and DAPI, revealed that 40.9 ± 0.4% of MM were within the endosteal region of C57Bl/6 BM (Figs. 1A, B). MM were counted based on size and morphology; c-Mpl stained green cells with a distinct and single nucleus, larger than three BM cell diameters were counted as MM. Based on our previous finding that 35.5 ±1.8% of extravascular BM cells are contained within the metaphyseal region of murine long bones (Ellis et al., 2011), plus taking into account the endosteal BM cells within 12 cell diameter of bone along the diaphysis, this represents a random MM distribution. However, analysis of stem and progenitor cell homing following transplant demonstrated a preferential lodgement near MM (Fig. 1C), with a significantly higher proportion of transplanted LSKSLAM cells (76.5 ± 2.2%; $p < 0.0001$) lodged within two cells of MM (Fig. 1D). Of these cells, ~70% were LSKSLAM isolated from the endosteal region and ~30% were LSKSLAM isolated from the central region (Fig. 1E). Together with our previously published data showing that LSKSLAM isolated from the endosteal region home more readily to the BM compared to their central counterparts, and endosteal LSKSLAM preferentially home back to the endosteal region (Grassinger et al., 2009), we deduce that endosteally isolated stem cells preferentially lodge near endosteal MM. The odds ratio, a mathematical measure of association, between MM (comprising ~0.2% of BM) and HSC (LSKSLAM comprising ~0.002% of BM (Grassinger et al., 2010)) co-localizing by chance is 2000 to 1. This close association between MM and HSC in the BM microenvironment suggests a possible functional interaction. To investigate the interaction between HSC and MM in vitro, we initially optimised a strategy for the prospective isolation of viable MM.

Viable MM can be isolated by FACS using CD41 and Hoechst33342

CD41, also known as glycoprotein (gp) IIb or integrin αIIb chain, associates with CD61 (gpIIIa or integrin β3 chain) to form the gpIIb/IIIa (CD41/CD61) complex expressed on

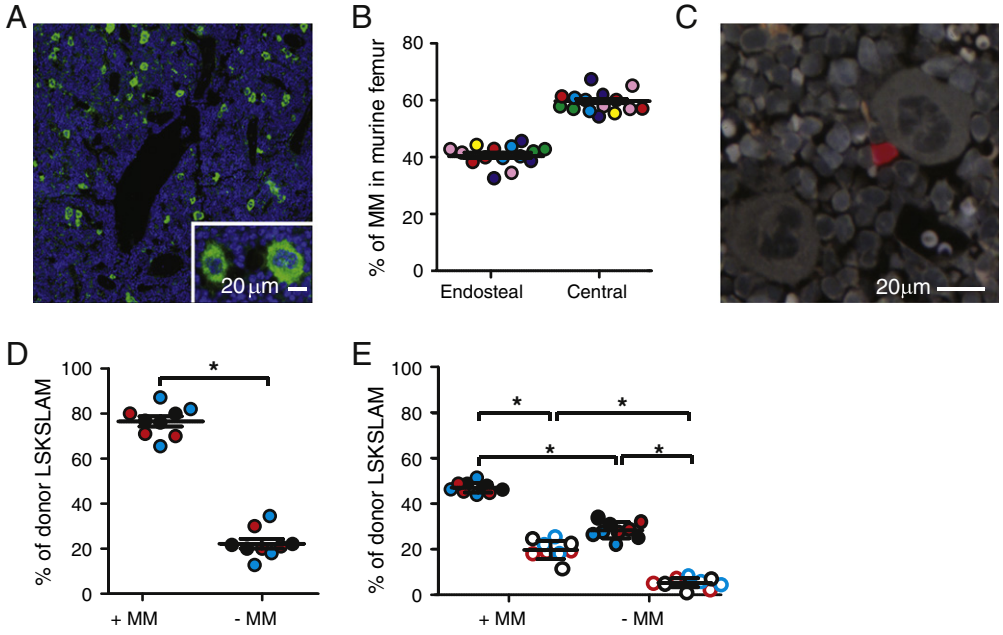

Figure 1 MM are randomly distributed and HSC preferentially lodge within two cells of MM 15 h post-transplant. (A) Longitudinal section of a C57Bl/6 femur stained with anti-c-Mpl (green) and DAPI (blue). (B) Megakaryocyte distribution based on analysis of c-Mpl$^+$ polyploidy MM. All cells within the trabaculae rich regions of the epi- and metaphyseal femoral regions, as well as cells within 12 cells of bone along the diaphyseal were classified as endosteal (individual replicates (n) = 15, biological repeats (r) = 6). At least 200 MM were scored per section. (C) Homed donor SNARF$^+$ stem cell (red) in direct contact with MM. (D) Proportion of donor LSKSLAM cells lodged within two cells of MM (+MM) or more than two cells from MM (−MM) ($p < 0.0001$) (n = 9, r = 3). Approximately 30 LSKSLAM cells were analysed per animal. (E) Proportion of donor LSKSLAM cells lodged within two cells of MM (+MM) or more than two cells from MM (−MM). Closed circles = LSKSLAM cells isolated from the endosteal BM region, open circles = LSKSLAM cells isolated from central BM ($p < 0.001$) (n = 9, r = 3). In all graphs each symbol represents an individual animal and each colour a biological repeat. All data are the mean ± SEM.

platelets, megakaryocytes, and early murine hemopoietic progenitors (Jennings & Phillips, 1982; Ferkowicz et al., 2003). MM can be isolated by FACS as SSC^{high}, CD41^{bright} cells (Figs. 2A, B) and sub-fractionated based on ploidy (Fig. 2C). From a total of 49 sorts, an average of 1756 8N MM (12.6% of total MM), 9109 16N MM (65.4% of total MM), 3035 32N MM (21.8% of total MM) and 32 64N MM (0.2% of total MM) were isolated from the femurs, tibias and iliac crests of a single mouse. The purity and viability of isolated MM were confirmed using microscopy, which revealed no contaminating cells, as well as RT-PCR. As expected, the expression of tubulin-β1, involved in megakaryocyte maturation, specifically pro-platelet formation and platelet release, significantly increased as megakaryocytes matured (Fig. 2D, $p = 0.02$). This confirmed the purity of our sorted ploidy populations. All MM populations tested showed constant minimal expression of Pu-1, a gene known to be key in myeloid and B-lymphoid cell commitment (data not shown).

Prospectively isolated megakaryocytes increase hemopoietic cell proliferation in vitro

To determine if MM influence hemopoietic cell proliferation, RFP$^+$ MM were co-cultured with C57Bl/6 LSKSLAM cells (Figs. 3A, B). While eLSKSLAM co-cultured with prospectively isolated MM showed increased stem cell proliferation (Fig. 3C, $p < 0.0001$), no significant difference was observed when HSC isolated from the central BM (cLSKSLAM) were co-cultured with MM (Fig. 3D). Previously, we demonstrated that HSC isolated from the endosteum have increased in vivo hemopoietic potential compared to their central counterparts (Grassinger et al., 2010; Haylock et al., 2007) and as a consequence, all further experimentation was conducted with LSKSLAM isolated from the endosteal region. Analysis of HSC progeny post-culture revealed no differences in the frequency of lineage committed cells; however, a significant increase in the absolute number of myeloid cells was detected (Figs. 3E, F, $p = 0.03$). Perhaps surprisingly, co-culture of individual ploidy MM with eLSKSLAM showed no significant increased hemopoietic cell proliferation (Fig. 3G, $p = 0.02$). To determine the hemopoietic capacity of co-culture progeny, we subsequently performed long-term limiting dilution transplant analysis.

Cultured HSC retain reconstitution capacity and multi-lineage potential

Limiting numbers of eLSKSLAM cells cultured for 6–7 days with or without MM were transplanted into lethally ablated recipients (Fig. 4A). Engraftment and multi-lineage reconstitution were measured in peripheral blood (PB) at 6 wks, 12 wks and 20 wks post-transplant, as well as in BM at 20 wks post-transplant, with the relative proportion of T cells (CD3$^+$), B cells (B220$^+$), myeloid cells (GR-1/Mac-1$^+$) and other cells assessed. While 1 in 26 starting eLSKSLAM cells cultured with MM were capable of long-term, multi-lineage reconstitution,

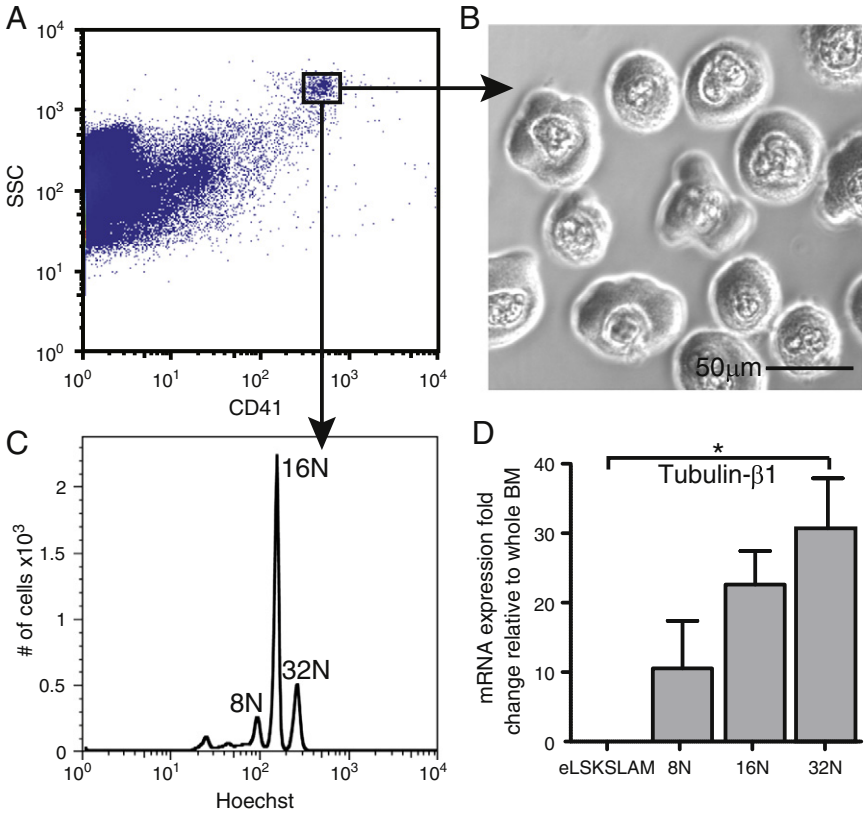

Figure 2 Isolation of viable MM using CD41 and Hoechst. (A) MM were identified as SSC^{high}CD41^{bright} cells. (B) Light microscope image of isolated MM. (C) Using Hoechst33342, MM were sub-fractionated based on ploidy (8N, 16N and 32N). (D) Tubulin-β1 mRNA expression in MM of individual ploidy, relative to B-actin ($n \geq 3$, $p = 0.02$, data is the mean ± SEM).

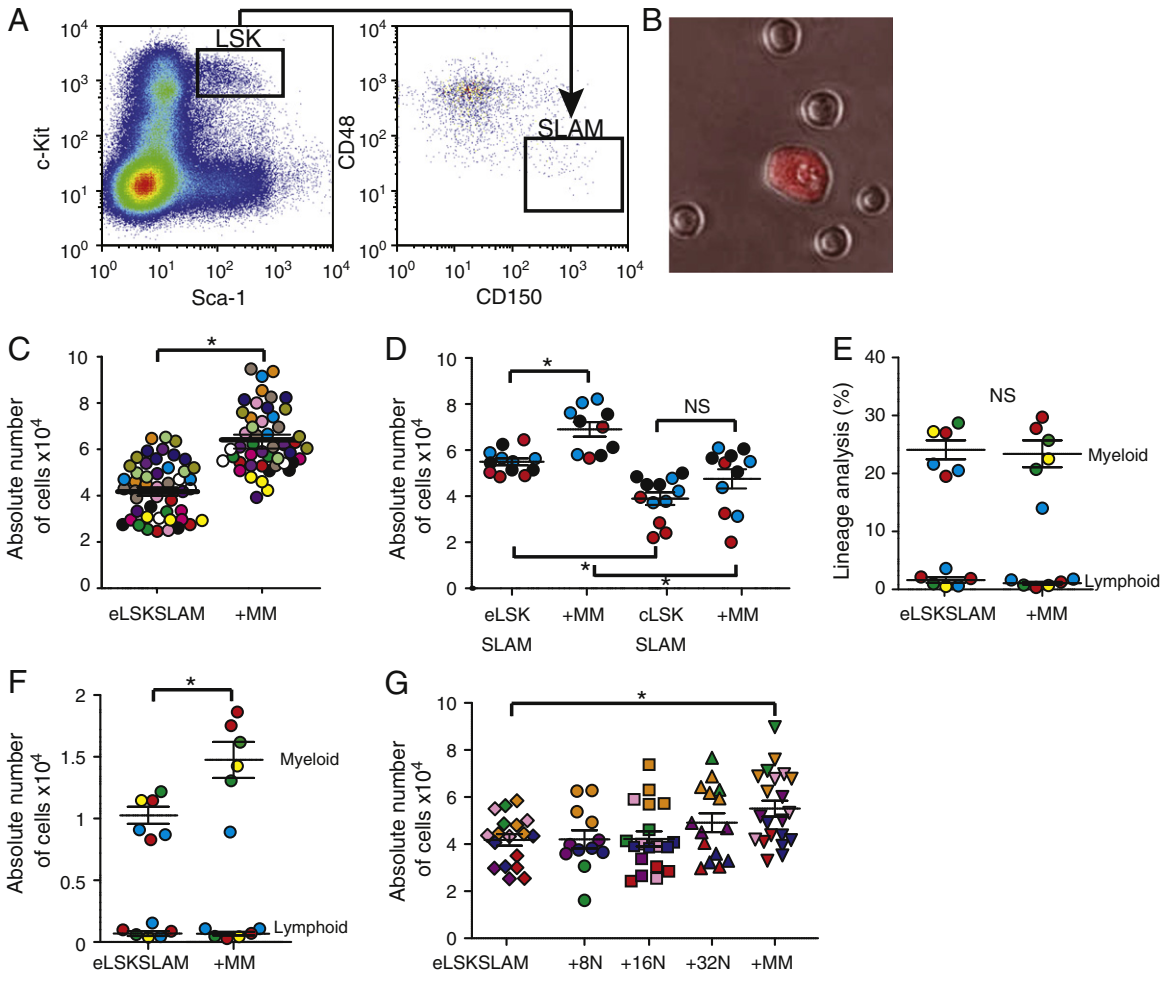

Figure 3 Prospectively isolated megakaryocytes increase endosteal hemopoietic cell proliferation in vitro. (A) Sorting strategy for the isolation of LSKSLAM cells. (B) RFP^+ MM were co-cultured 6–7 days with C57Bl/6 LSKSLAM cells (image was taken with a 10× objective). (C) Progeny of eLSKSLAM cultures with and without MM ($p < 0.0001$) (individual replicates (n) $\geq$ 36, biological repeats (r) = 11). (D) Progeny of cLSKSLAM cultures with and without MM, compared to eLSKSLAM cells ($p > 0.05$) ($n \geq 11$, r = 3). (E) Lineage analysis of cells post-culture with or without MM. Myeloid = $Gr\text{-}1^+/Mac\text{-}1^+$, lymphoid = $B220^+/CD3^+$ (n = 6, r = 4). (F) Absolute numbers of cells post-culture with or without MM. Myeloid = $Gr\text{-}1^+/Mac\text{-}1^+$, lymphoid = $B220^+/CD3^+$ (n = 6, r = 4, $p = 0.026$). (G) eLSKSLAM co-cultured with MM of individual ploidy ($p = 0.02$) ($n \geq 12$, $r \geq 4$). In all graphs, each colour represents an independent experiment; dots of the same colour represent replicates within the same experiment. All data is the mean ± SEM.

only 1 in 39 starting eLSKSLAM cells cultured alone possessed the same potential (Fig. 4B). However, this difference in frequency was not significantly different. In experiments where 10 starting cell equivalents were transplanted; MM co-cultured eLSKSLAM cells showed significantly increased long-term multi-lineage reconstitution in lethally ablated mice (Fig. 4B, $p < 0.05$). Therefore, co-culture with MM resulted in both the expansion of cells with multi-lineage reconstitution potential as well as hemopoietic cell differentiation. This difference in potential was only evident following the transplant of limiting numbers of cells, allowing subtle differences in reconstituting potential to be revealed. These findings are similar to those previously reported for transplants into altered hemopoietic microenvironments (Nilsson et al., 2005).

Both eLSKSLAM cultured alone or with MM demonstrated long-term multi-lineage reconstitution of lethally ablated recipients, with steady-state proportions of each cell type evident at all time points after transplants of the progeny of between 10 and 100 eLSKSLAM (Figs. 4C, D). These results were equivalent to our previously published data showing lineage commitment of transplanted eLSKSLAM cells (Grassinger et al., 2010). Together, these findings demonstrate that MM significantly increased the proliferation of lineage committed cell as well as hemopoietic cells with reconstitution potential. Next, we investigated the mechanism underpinning this MM stimulated increase in proliferation.

Megakaryocytes release IGF-1 and IGFBP-3 which increase hemopoietic cell proliferation through the IGF-1R

In order to determine if the observed increased proliferation was contact-dependent, we cultured eLSKSLAM in MM-CM.

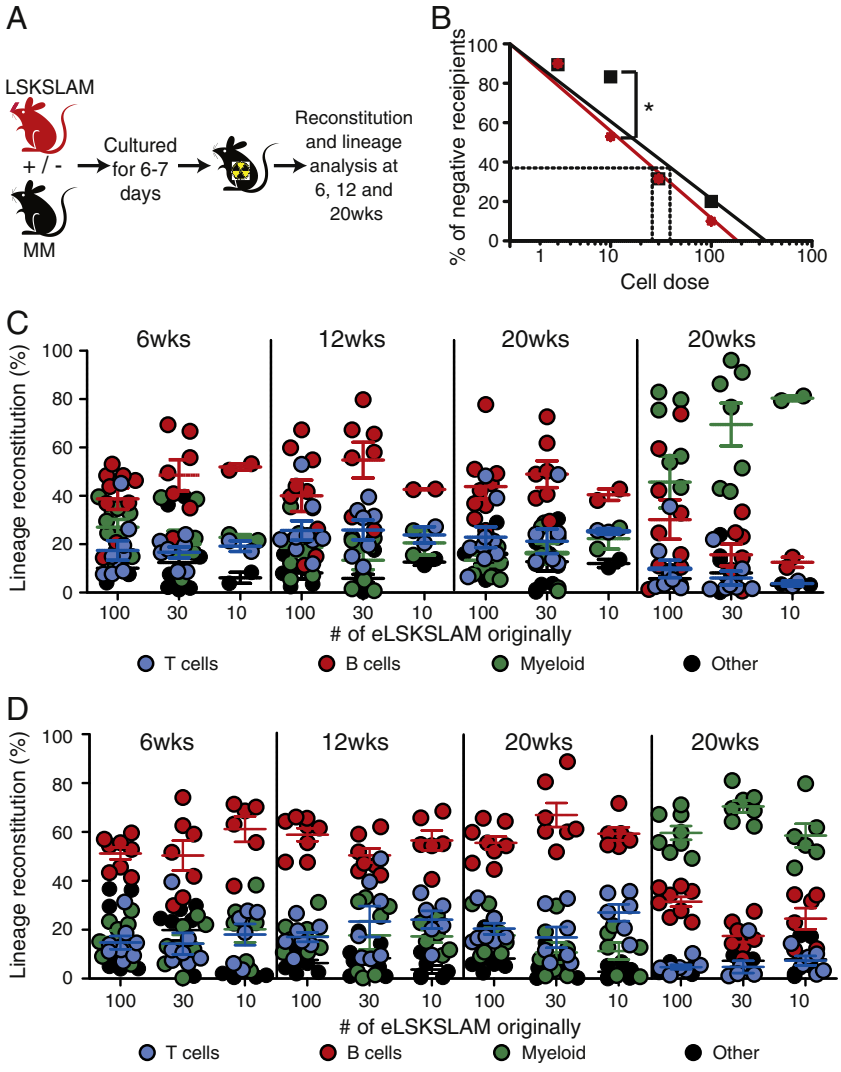

Figure 4 Cultured HSC retain reconstitution ability and multi-lineage potential. (A) Schematic of transplant assay. (B) Incidence of long-term repopulating cells from eLSKSLAM cells cultured alone (black) or with MM (red) (for 10 starting cell equivalents only, $p < 0.05$) (individual replicates (n) ≥ 10, biological repeats (r) ≥ 2). (C, D) PB and BM donor lineage reconstitution following transplants of progeny of eLSKSLAM cells cultured alone (C) or with MM (D) ($n \geq 10$, $r \geq 2$). Cells were identified as B cells ($B220^+$), T cells ($CD3^+$), myeloid cells ($Gr\text{-}1^+/Mac\text{-}1$) or other cells (non-lymphoid or myeloid cells).

No difference was detected in the proliferation of eLSKSLAM in MM-CM compared to co-culture with MM, with a significant increase in proliferation compared to cultured eLSKSLAM alone (Fig. 5A, $p < 0.001$), demonstrating that increased proliferation is not due to cell–cell interactions. A custom cytokine array analysis highlighted multiple factors released by MM (IGF-2 and IGFBP-2) which have previously been shown to impact HSC proliferation in vitro (Zhang & Lodish, 2004; Huynh et al., 2008, 2011), as well as other IGF and IGFBP family members (IGF-1 and IGFBP-3) (Fig. 5B). qRT-PCR confirmed MM transcribe IGF-1 and IGFBP-3 mRNA (Fig. 5C) and immunohistochemical analysis confirmed IGFBP-3 protein expression in situ (Fig. 5D). The presence of IGFBP-3 in BM fluid as well as its release from prospectively isolated MM into culture media was also evident immunohistochemically and confirmed by ELISA (Figs. 5D, E, F). However, the fact that IGFBP-3 transcript could only be detected in very high ploidy MM, but equivalent protein was released from MM of other ploidy suggests that this factor is being endocytosed and sequestered for later release, a process of cytokine storage previously described for this cell type (Chan & Spencer, 1998).

Culture studies of eLSKSLAM in media supplemented with IGFBP-3 alone, IGF-1 alone or IGF-1 and IGFBP-3 reproduced the increased hemopoietic cell proliferation evident in HSC cultures with MM, in an additive, IGFBP-3 dose dependent manner (Fig. 5G, $p < 0.001$). Post-culture analysis showed no difference in lineage commitment between eLSKSLAM cells cultured alone or cultured with IGF-1 and IGFBP-3 (data not shown). In addition, this IGF-1 and IGFBP-3 induced hemopoietic cell proliferation could be inhibited by a neutralising anti-IGF-1 antibody (Fig. 5H, $p < 0.001$). These data suggest that IGFBP-3 is regulating HSC both independently, as well as in conjunction with IGF-1. To elucidate the mechanism by which IGF-1/IGFBP-3 regulates hemopoietic cell proliferation, we examined HSC for two receptors to which IGF-1 and potentially IGFBP-3 are known to bind: IGF-1

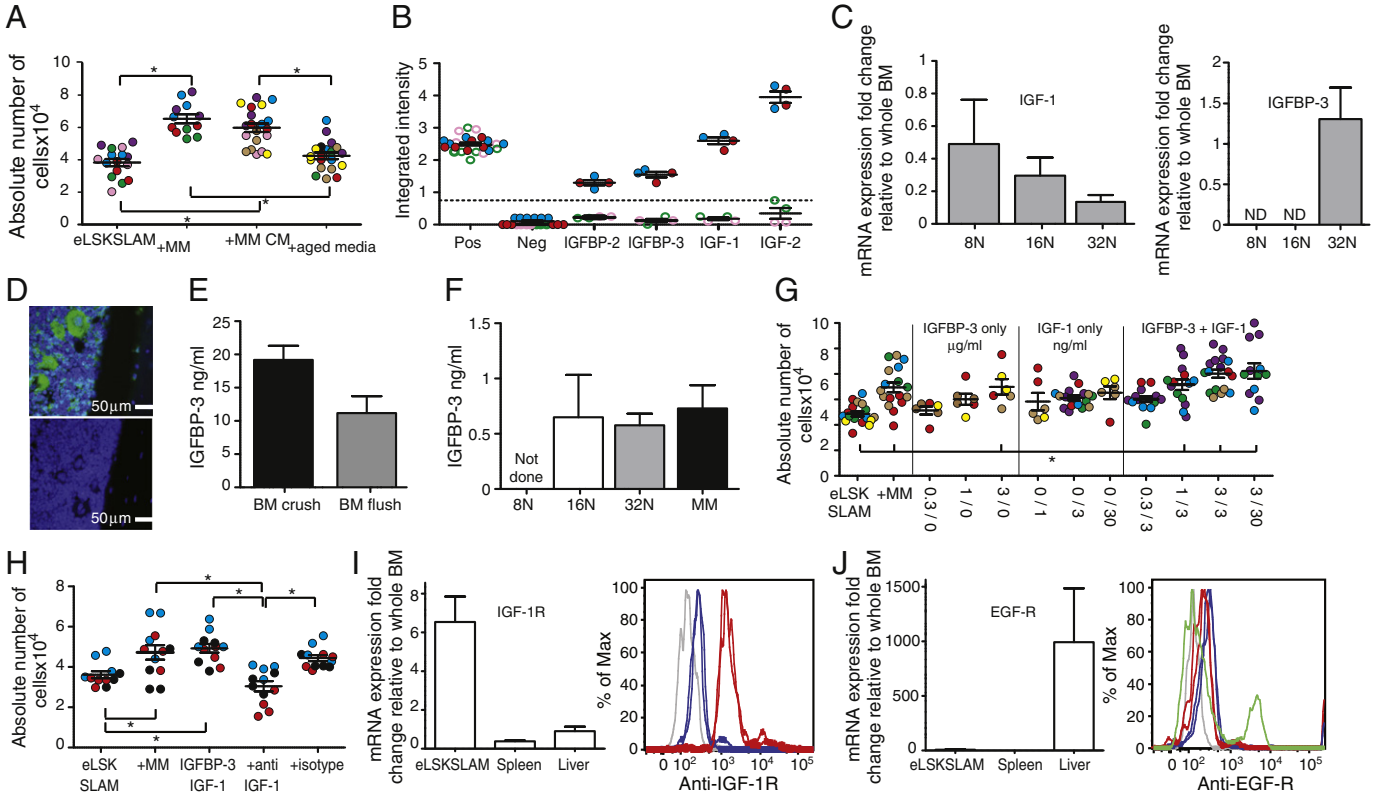

Figure 5 Megakaryocytes release IGF-1 and IGFBP-3 which increase hemopoietic cell proliferation through IGF-R. (A) Progeny of eLSKSLAM cultured in MM-CM ($p < 0.05$).(individual replicates (n) $\geq$ 12, biological repeats (r) $\geq$ 4). (B) Factors released by MM detected by a custom mouse cytokine array (n = 4, r = 2). Pos and neg = ELISA kit controls. Closed circles = MM-conditioned media, open circles = media only control. (C) Analysis of IGF-1 and IGFBP-3 mRNA expression in different MM ploidy populations, relative to B-actin (n $\geq$ 3, ND = not detected). (D) IGFBP-3 protein expression in BM section, isotype control below (n $\geq$ 3). (E) IGFBP-3 in BM detected by ELISA (n $\geq$ 2). (F) IGFBP-3 released into culture media by MM of individual ploidy detected by ELISA (n $\geq$ 2). Due to low cell recovery, 8N MM were not tested. (G) Progeny of eLSKSLAM cells in media supplemented with different concentrations of IGFBP-3, IGF-1 or both factors together ($p < 0.05$) (n $\geq$ 6, r $\geq$ 3). IGFBP-3 (µg/ml)/IGF-1 (ng/ml) concentrations. (H) Analysis of neutralising anti-IGF-1 antibody on eLSKSLAM cells cultured in media supplemented with IGF-1 and IGFBP-3 ($p < 0.05$) (n $\geq$ 11, r = 3). (I) Analysis of IGF-1R transcript and protein expression on HSC (n $\geq$ 3, r $\geq$ 2). Grey = unstained, blue = isotype, red = antibody. (J) Analysis of EGF-R transcript and protein expression on HSC (n $\geq$ 3, r $\geq$ 2). Grey = unstained, blue = isotype, red = antibody, green = positive control. In all graphs, each colour represents an independent experiment; dots of the same colour represent replicates within the same experiment. All data is the mean ± SEM.

receptor (IGF-1R) and epidermal growth factor receptor (EGF-R) (Martin & Baxter, 2011; Mohseni-Zadeh & Binoux, 1997). HSC demonstrated high mRNA and protein expression for IGF-1R but undetectable expression of EGF-R (Figs. 5I, J). Together, the data suggests that IGF-1 and IGFBP-3 released from MM act through the IGF-1R to mediate hemopoietic cell proliferation.

Discussion

We report that while MM are randomly distributed within BM, 15-h post-transplant, HSC (LSKSLAM cells) preferentially home to be within two cells of MM. To investigate whether these two cell types could influence the biology of the other, we refined a FACS based method for prospectively isolating $CD41^+$ MM, yielding a significant number of pure, viable 8N, 16N, 32N and 64N cells, allowing the assessment of MM and HSC interactions in vitro. Sorted MM were intact and bright under phase contrast pre- and post-culture. Previous methods for isolating MM and their limitations are discussed in our detailed chapter on the prospective isolation of viable MM (Heazlewood et al., 2013). Our HSC/MM co-culture studies showed that prospectively isolated MM significantly increased the proliferation of hemopoietic cells, with an expansion of cells with multi-lineage reconstitution potential as well as differentiated hemopoietic cells. Our data also showed that the MM stimulatory effect of hemopoietic cell proliferation is not cell contact-dependent, but the proliferative stimulus is mediated by the additive effect of released IGF-1 and IGFBP-3, which can be inhibited by a neutralising anti-IGF-1 antibody. We also showed that HSC express IGF-1R.

While a recent review highlighted a number of papers identifying IGFBP-3 as an inhibitor of proliferation (Martin & Baxter, 2011), there are numerous studies implicating IGFBP-3, both alone and in conjunction with IGF-1, in stimulating cell proliferation. IGFBP-3 can stimulate cell proliferation by activation of sphingosine kinase-1, leading to the production of sphingosine-1-phosphate and transactivation of IGF-1R (Martin et al., 2009). Furthermore, IGFBP-3 can activate IGF-1R via the phosphatidylinositol-3 kinase pathway (Conover et al., 2000). Interestingly, there is evidence supporting IGFBP-3 directly interacting with IGF-1R (Mohseni-Zadeh & Binoux, 1997). In addition, it has also been reported that IGFBP-3 independently mediates TGF-β-induced smooth muscle cell and carcinoma cell proliferation (Cohen et al., 2000; Kansra et al., 2000), with TGF-β known to be stored and released by megakaryocytes (Fava et al., 1990). Furthermore, IGFBP-3 has been shown to synergise with Jagged-1 and Delta-1 to increase HSC proliferation (Liu et al., 2003).

IGFBP-3 and acid-labile subunit are able to sequester IGF-1 to increase the half-life of IGF-1 from 10 min to 15 h (Guler et al., 1989; Baxter, 1994). This could account for the non-significant increase in proliferation when eLSKSLAM were cultured in IGF-1 alone; without IGFBP-3 to prolong the activity of IGF-1, eLSKSLAM received no additional signal to increase their proliferation. However, in the presence of IGF-1 and IGFBP-3, both IGF-1 direct and indirect mechanisms appear to induce hemopoietic cell proliferation.

Whilst we demonstrate that IGF-1 and IGFBP-3 increase hemopoietic cell proliferation, we cannot exclude the role of other IGF and IGFBP family members. For example, IGFBP-2, -4, -5 and -6 in conjunction with, or independent of IGFs may regulate hemopoietic stem and progenitor cell migration and/or proliferation (Grellier et al., 1995; Bartling et al., 2010). Furthermore, endogenous or exogenous IGFBP-2 and IGF-2 have previously been shown to stimulate HSC proliferation (Zhang & Lodish, 2004; Huynh et al., 2008, 2011). We now demonstrate that MM release IGF-2 and IGFBP-2 into the environment and therefore may potentially regulate HSC via this mechanism. While, our IGF-1 neutralising antibody ameliorated the additive IGF-1 and IGFBP-3 induced increase in hemopoietic cell proliferation in vitro, its ability to modify the actions of other IGF and IGFBP family members remains unclear.

We report that LSKSLAM cells isolated from the central BM region do not show significantly increased proliferation when co-cultured with MM, despite MM being randomly distributed throughout the marrow and HSC and MM co-localizing post-transplant. Furthermore, no difference in IGF1-R expression between LSKSLAM cells isolated from the central or endosteal region was detected (data not shown). This difference in effects on HSC isolated from the endosteal versus central BM regions is consistent with our previously published work demonstrating that although phenotypically identical for lineage, Sca-1, c-Kit, CD150 and CD48 expression, stem cells isolated from different regions of the BM have different functional potential both in vitro and in vivo (Grassinger et al., 2010; Haylock et al., 2007). These functional differences are likely to be due to a combination of intrinsic and other extrinsic microenvironmental influences. Our data demonstrates that in the presence of MM, HSC isolated from the endosteal region retain their natural ability to proliferate faster than their central counterpart. However, in the presence of MM, this increased proliferation is amplified because MM release additional stimulatory signals.

Interestingly, our data showed that when eLSKSLAM were co-cultured with individual ploidy MM, the significant increase in proliferation was no longer observed. In addition, we observed less than expected proliferation when eLSKSLAM cells were co-cultured with MM that had been stained with Hoechst33342 (Fig. 3G compared to Fig. 3C). This could be due to Hoechst33342 interfering with MM induced hemopoietic cell proliferation as it is known that Hoechst33342 can cause cytotoxicity and affect cell cycling (Wiezorek, 1984; Erba et al., 1988). Our experiments revealed that only 32N MM, not 8N or 16N MM, express IGFBP-3 transcript; while 8N MM express more IGF-1 transcript than 16N or 32N MM. Therefore, different ploidy populations may contribute differently to affect eLSKSLAM cell proliferation. However, ELISA data showed that compared to 32N MM, and despite having no detectable IGFBP-3 transcript, 16N MM released similar quantities of IGFBP-3 into culture media. It has previously been shown that MM endocytose and store IGF-1 and IGFBP-3 in platelet α-granules (Chan & Spencer, 1998). As we very rarely observed pro-platelet formation and platelets during MM cultures, release of these cytokines from platelets would not have impacted on our results. Taken together, it is possible that 32N MM produce endogenous IGFBP-3 as well as endocytose IGFBP-3 from the environment, and this could account for the slight but non-significant increase in hemopoietic cell proliferation while in co-culture with 32N MM. Other factors may also be involved and therefore, more experimentation is required to determine any importance of ploidy in hemopoietic cell proliferation.

Our hypothesis that MM regulate HSC is also supported by several other studies. Umbilical cord blood (UCB) differentiated CD41$^+$ megakaryocytes have a stimulatory effect on UCB stem cells by promoting the proliferation of long-term culture initiating cells (Kirouac et al., 2010). In addition, MM produce the known HSC regulator IL-6 (Suzuki et al., 1989; Jiang et al., 1994). MM also influence HSC indirectly by regulating OB (via $\alpha_3\beta_1$, $\alpha_5\beta_1$ and CD41), which in turn, regulate HSC (Lemieux et al., 2010). This is potentially mediated through GATA-1; because GATA-1 deficient mice have increased numbers of megakaryocytes as well as increased bone mass (Ciovacco et al., 2010). MM are a major source of factors such as thrombospondin, platelet-derived growth factor, basic fibroblast growth factor-2, bone morphogenic proteins-2, -4 and -6, receptor activator for nuclear factor κ B ligand, osteocalcin, osteonectin, osteopontin, osteoprotegerin and bone sialoprotein, which are important in the regulation of bone homeostasis, HSC, as well as recovery of the vasculature and OB following BM damage (Kacena et al., 2006; Kopp et al., 2006; Dominici et al., 2009). Therefore, the fact that megakaryocytes secrete many cytokines that influence the proliferation and survival of not only HSC and other hemopoietic cell types, but also bone formation, highlights their key regulatory role and identifies them as a potential niche component.

In conclusion, our data suggests that MM regulate HSC via cytokine release. MM are randomly distributed within the BM, but HSC preferentially lodge within two cells of MM post-transplant. MM increase hemopoietic cell proliferation in vitro via the release of IGF-1 and IGFBP-3. This strongly implicates this mature hemopoietic cell type, primarily responsible for platelet production, as actively contributing to HSC regulation by providing signals that not only maintain and induce stem cell proliferation, but also influence the make-up of the BM microenvironment.

Authorship contributions

S.H. and S.N. designed and performed experiments, analysed data and wrote the manuscript. R.N. designed and performed experiments, analysed data and assessed the manuscript. B.W. was fundamental in developing prospective MM ploidy cell separation and performed experiments. D.H. designed experiments and critically analysed the manuscript. T.A. provided intellectual input underpinning experimental design, supplied reagents and critically analysed the manuscript.

Disclosure of conflict of interest

The authors have no conflicts of interest to disclose.

Acknowledgments

This work was supported by grants from the Australian Stem Cell Centre to S.N. We thank Chad Heazlewood, Andrea Reitsma and Songhui Li for technical assistance, Daniela Cardozo for assistance with animal work, Robert Baxter for intellectual input, Dave Winkler for assistance with statistical analysis, Peter McCourt for critically assessing the manuscript, Patrick Tam for RFP mice and Jochen Grassinger for providing image 1C. We also thank Andrew Fryga, Michael Reitsma, Kathryn Flanagan and Karen Clarke for flow cytometric support.

References

Bartling, B., Koch, A., Simm, A., Scheubel, R., Silber, R.E., Santos, A.N., 2010. Insulin-like growth factor binding proteins-2 and -4 enhance the migration of human CD34−/CD133+ hematopoietic stem and progenitor cells. Int. J. Mol. Med. 25 (1), 89–96.

Baxter, R.C., 1994. Insulin-like growth factor binding proteins in the human circulation: a review. Horm. Res. 42 (4–5), 140–144.

Beeton, C.A., Bord, S., Ireland, D., Compston, J.E., 2006. Osteoclast formation and bone resorption are inhibited by megakaryocytes. Bone 39 (5), 985–990.

Bord, S., Frith, E., Ireland, D.C., Scott, M.A., Craig, J.I., Compston, J.E., 2005. Megakaryocytes modulate osteoblast synthesis of type-I collagen, osteoprotegerin, and RANKL. Bone 36 (5), 812–819.

Chan, K., Spencer, E.M., 1998. Megakaryocytes endocytose insulin-like growth factor (IGF) I and IGF-binding protein-3: a novel mechanism directing them into alpha granules of platelets. Endocrinology 139 (2), 559–565.

Ciovacco, W.A., Cheng, Y.H., Horowitz, M.C., Kacena, M.A., 2010. Immature and mature megakaryocytes enhance osteoblast proliferation and inhibit osteoclast formation. J. Cell. Biochem. 109 (4), 774–781.

Cohen, P., Rajah, R., Rosenbloom, J., Herrick, D.J., 2000. IGFBP-3 mediates TGF-beta1-induced cell growth in human airway smooth muscle cells. Am. J. Physiol. Lung Cell. Mol. Physiol. 278 (3), L545–L551.

Conover, C.A., Bale, L.K., Durham, S.K., Powell, D.R., 2000. Insulin-like growth factor (IGF) binding protein-3 potentiation of IGF action is mediated through the phosphatidylinositol-3-kinase pathway and is associated with alteration in protein kinase B/AKT sensitivity. Endocrinology 141 (9), 3098–3103.

Dominici, M., Rasini, V., Bussolari, R., et al., 2009. Restoration and reversible expansion of the osteoblastic hematopoietic stem cell niche after marrow radioablation. Blood 114 (11), 2333–2343.

Ellis, S.L., Grassinger, J., Jones, A., et al., 2011. The relationship between bone, hemopoietic stem cells, and vasculature. Blood 118 (6), 1516–1524.

Erba, E., Ubezio, P., Broggini, M., Ponti, M., D'Incalci, M., 1988. DNA damage, cytotoxic effect and cell-cycle perturbation of Hoechst 33342 on L1210 cells in vitro. Cytometry 9 (1), 1–6.

Fava, R.A., Casey, T.T., Wilcox, J., Pelton, R.W., Moses, H.L., Nanney, L.B., 1990. Synthesis of transforming growth factor-beta 1 by megakaryocytes and its localization to megakaryocyte and platelet alpha-granules. Blood 76 (10), 1946–1955.

Ferkowicz, M.J., Starr, M., Xie, X., et al., 2003. CD41 expression defines the onset of primitive and definitive hematopoiesis in the murine embryo. Development 130 (18), 4393–4403.

Grassinger, J., Haylock, D.N., Storan, M.J., et al., 2009. Thrombin-cleaved osteopontin regulates hemopoietic stem and progenitor cell functions through interactions with alpha9beta1 and alpha4beta1 integrins. Blood 114 (1), 49–59.

Grassinger, J., Haylock, D.N., Williams, B., Olsen, G.H., Nilsson, S.K., 2010. Phenotypically identical hemopoietic stem cells isolated from different regions of bone marrow have different biologic potential. Blood 116 (17), 3185–3196.

Grellier, P., Yee, D., Gonzalez, M., Abboud, S.L., 1995. Characterization of insulin-like growth factor binding proteins (IGFBP) and regulation of IGFBP-4 in bone marrow stromal cells. Br. J. Haematol. 90 (2), 249–257.

Guler, H.P., Zapf, J., Schmid, C., Froesch, E.R., 1989. Insulin-like growth factors I and II in healthy man. Estimations of half-lives and production rates. Acta Endocrinol. (Copenh) 121 (6), 753–758.

Haylock, D.N., Williams, B., Johnston, H.M., et al., 2007. Hemopoietic stem cells with higher hemopoietic potential reside at the bone marrow endosteum. Stem Cells 25 (4), 1062–1069.

Heazlewood, S.Y., Williams, B., Storan, M.J., Nilsson, S.K., 2013. The prospective isolation of viable, high ploidy megakaryocytes from adult murine bone marrow by fluorescence activated cell sorting. In: Turksen, K. (Ed.), Stem Cell Niche: Methods and Protocols, Methods in Molecular Biology, vol. 1035. Springer Science + Business Media LLC, USA.

Huynh, H., Iizuka, S., Kaba, M., et al., 2008. Insulin-like growth factor-binding protein 2 secreted by a tumorigenic cell line supports ex vivo expansion of mouse hematopoietic stem cells. Stem Cells 26 (6), 1628–1635.

Huynh, H., Zheng, J., Umikawa, M., et al., 2011. IGF binding protein 2 supports the survival and cycling of hematopoietic stem cells. Blood 118 (12), 3236–3243.

Jennings, L.K., Phillips, D.R., 1982. Purification of glycoproteins IIb and III from human platelet plasma membranes and characterization of a calcium-dependent glycoprotein IIb–III complex. J. Biol. Chem. 257 (17), 10458–10466.

Jiang, S., Levine, J.D., Fu, Y., et al., 1994. Cytokine production by primary bone marrow megakaryocytes. Blood 84 (12), 4151–4156.

Kacena, M.A., Shivdasani, R.A., Wilson, K., et al., 2004. Megakaryocyte–osteoblast interaction revealed in mice deficient in transcription factors GATA-1 and NF-E2. J. Bone Miner. Res. 19 (4), 652–660.

Kacena, M.A., Nelson, T., Clough, M.E., et al., 2006. Megakaryocyte-mediated inhibition of osteoclast development. Bone 39 (5), 991–999.

Kansra, S., Ewton, D.Z., Wang, J., Friedman, E., 2000. IGFBP-3 mediates TGF beta 1 proliferative response in colon cancer cells. Int. J. Cancer 87 (3), 373–378.

Kirouac, D.C., Ito, C., Csaszar, E., et al., 2010. Dynamic interaction networks in a hierarchically organized tissue. Mol. Syst. Biol. 6, 417.

Kopp, H.G., Hooper, A.T., Broekman, M.J., et al., 2006. Thrombospondins deployed by thrombopoietic cells determine angiogenic switch and extent of revascularization. J. Clin. Invest. 116 (12), 3277–3291.

Lemieux, J.M., Horowitz, M.C., Kacena, M.A., 2010. Involvement of integrins alpha(3)beta(1) and alpha(5)beta(1) and glycoprotein IIb in megakaryocyte-induced osteoblast proliferation. J. Cell. Biochem. 109 (5), 927–932.

Liu, L.Q., Sposato, M., Liu, H.Y., et al., 2003. Functional cloning of IGFBP-3 from human microvascular endothelial cells reveals its novel role in promoting proliferation of primitive CD34 + CD38- hematopoietic cells in vitro. Oncol. Res. 13 (6–10), 359–371.

Martin, J.L., Baxter, R.C., 2011. Signalling pathways of insulin-like growth factors (IGFs) and IGF binding protein-3. Growth Factors 29 (6), 235–244.

Martin, J.L., Lin, M.Z., McGowan, E.M., Baxter, R.C., 2009. Potentiation of growth factor signaling by insulin-like growth factor-binding protein-3 in breast epithelial cells requires sphingosine kinase activity. J. Biol. Chem. 284 (38), 25542–25552.

Mohseni-Zadeh, S., Binoux, M., 1997. Insulin-like growth factor (IGF) binding protein-3 interacts with the type 1 IGF receptor, reducing the affinity of the receptor for its ligand: an alternative mechanism in the regulation of IGF action. Endocrinology 138 (12), 5645–5648.

Nakamura-Ishizu, A., Okuno, Y., Omatsu, Y., et al., 2012. Extracellular matrix protein tenascin-C is required in the bone marrow microenvironment primed for hematopoietic regeneration. Blood 119 (23), 5429–5437.

Nilsson, S.K., Dooner, M.S., Tiarks, C.Y., Weier, H.U., Quesenberry, P.J., 1997. Potential and distribution of transplanted hematopoietic stem cells in a nonablated mouse model. Blood 89 (11), 4013–4020.

Nilsson, S.K., Haylock, D.N., Johnston, H.M., Occhiodoro, T., Brown, T.J., Simmons, P.J., 2003. Hyaluronan is synthesized by primitive hemopoietic cells, participates in their lodgment at the endosteum following transplantation, and is involved in the regulation of their proliferation and differentiation in vitro. Blood 101 (3), 856–862.

Nilsson, S.K., Johnston, H.M., Whitty, G.A., et al., 2005. Osteopontin, a key component of the hematopoietic stem cell niche and regulator of primitive hematopoietic progenitor cells. Blood 106 (4), 1232–1239.

Schofield, R., 1978. The relationship between the spleen colony-forming cell and the haemopoietic stem cell. Blood Cells 4 (1–2), 7–25.

Shen, Y., Nilsson, S.K., 2012. Bone, microenvironment and hematopoiesis. Curr. Opin. Hematol. 19 (4), 250–255.

Smith, L.H., Clayton, M.L., 1970. Distribution of injected 59Fe in mice. Exp. Hematol. 20, 82–86.

Stier, S., Ko, Y., Forkert, R., et al., 2005. Osteopontin is a hematopoietic stem cell niche component that negatively regulates stem cell pool size. J. Exp. Med. 201 (11), 1781–1791.

Suzuki, C., Okano, A., Takatsuki, F., et al., 1989. Continuous perfusion with interleukin 6 (IL-6) enhances production of hematopoietic stem cells (CFU-S). Biochem. Biophys. Res. Commun. 159 (3), 933–938.

Twigg, S.M., Hardman, K.V., Baxter, R.C., 2000. A purified bovine serum albumin preparation contains an insulin-like growth factor (IGF) binding protein-3 fragment that forms ternary complexes selectively with IGF-II and the acid-labile subunit. Growth Horm. IGF Res. 10 (4), 215–223.

Wiezorek, C., 1984. Cell cycle dependence of Hoechst 33342 dye cytotoxicity on sorted living cells. Histochemistry 81 (5), 493–495.

Winter, O., Moser, K., Mohr, E., et al., 2010. Megakaryocytes constitute a functional component of a plasma cell niche in the bone marrow. Blood 116 (11), 1867–1875.

Zhang, C.C., Lodish, H.F., 2004. Insulin-like growth factor 2 expressed in a novel fetal liver cell population is a growth factor for hematopoietic stem cells. Blood 103 (7), 2513–2521.